Numerical Analysis of Bifilar Coil Geometry on Induction Heating Performance for Self-healing Asphalt

Jaka Sulistya Budi
Department of Mechanical Engineering, Universitas Sebelas Maret

Ubaidillah
Department of Mechanical Engineering, Universitas Sebelas Maret

Aditya Rio Prabowo
Department of Mechanical Engineering, Universitas Sebelas Maret

Esdiyanto, Ardi
Department of Mechanical Engineering, Universitas Sebelas Maret

他

https://doi.org/10.5109/6782164

出版情報：Evergreen. 10 (1), pp.574-584, 2023-03. 九州大学グリーンテクノロジー研究教育センター
バージョン：

Numerical Analysis of Bifilar Coil Geometry on Induction Heating Performance for Self-healing Asphalt

Jaka Sulistya Budi[1], Ubaidillah[1,2*], Aditya Rio Prabowo[1], Ardi Esdiyanto[1], Zainal Arifin[1], Zilmy Efis Priyatama[1]

[1]Department of Mechanical Engineering, Universitas Sebelas Maret, Surakarta 57126, Indonesia

[2]Department of Mechanical Engineering, Islamic University of Madinah, Medina, 42351, Saudi Arabia

* Corresponding Author Email: ubaidillah_ft@staff.uns.ac.id

(Received February 27, 2023; Revised March 24, 2023; accepted March 24, 2023).

Abstract: This paper proposes a bifilar coil numerical analysis for asphalt induction heating. The software utilized in this research was ANSYS Electronics Desktop and ANSYS Transient Analysis. The asphalt has been modified by adding a certain amount of iron flakes. The asphalt containing magnetic substances is modeled and subjected to an electromagnetic field, thus a comparative temperature distribution between bifilar and monofilar coils is achieved. The bifilar coil has a slight increase in output than the monofilar coil under conditions of equal current and frequency. However, bifilar coil provides less power consumption and self-capacitance compared to the counterpart.

Keywords: induction heating, asphalt, self-healing, monofilar, bifilar, numerical analysis

1. Introduction

Asphalt is the most prevalent type of pavement due to its advantages, which include a comfortable driving experience, great cost-efficiency, and superior noise reduction compared to other options.[1), 2), 3)]. In the past few decades, asphalt roads have dominated the transportation system. It is estimated that the asphalt road network is about 516,239 kilometers long. It has also gained the leading position in regional economic development and commerce[4)]. As time passes, the asphalt will begin to crack due to its constant exposure to a variety of environmental factors, such as rainwater, chemical fluids, fluctuating temperatures, etc., which will reduce its durability[5)]. To protect the environment and cut down on the consumption of nonrenewable natural resources, numerous initiatives have been taken, one of which is to make asphalt last as long as it possibly can[6)].

When a material can repair its damage, it is referred to a self-healing material which is defined as the capacity of a material to automatically repair any damage it may have sustained without requiring assistance from an outside source. The level of damage that can be sustained is minimized while, at the same time, the material's useful life is increased through self-healing. The objective is to reduce the level of deterioration and increase the service life[7)]. The self-healing material exhibited a different behavior to that of conventional material. The conventional materials suffer wear and tear over time and become unusable after a certain amount of time. Materials that are improvised, on the other hand, adhere to the same principle but have a momentary extension of time. Self-healing materials, on the other hand, may initially sustain minor damage, but their service life will be significantly prolonged until they have sustained total damage[8), 9)].

Researchers predict that sealing microcracks will improve the service life of asphalt[10), 11)]. Microcracks are tiny cracks that are not visible to the naked eye but can have a significant impact on the overall integrity of the asphalt. Microcracks can be caused by a variety of factors, including temperature fluctuations, aging, and traffic loads. They can lead to the degradation of the asphalt, reducing its lifespan and increasing maintenance costs. If left untreated, microcracks can also lead to more significant types of cracking, such as alligator cracking. To prevent microcracks, it is essential to ensure that the asphalt is properly designed and constructed for the anticipated traffic loads and environmental conditions. Regular maintenance, such as filling in any visible cracks, can also help prevent the formation of microcracks. In some cases, techniques such as crack sealing or micro-surfacing may be used to prevent the spread of microcracks and extend the life of the asphalt.

Various approaches, such as encapsulated rejuvenators [12)], microvascular fibers[13)], microwave heating[14)], and induction heating[15)], have been researched to achieve the self-healing phase. Temperature is the most crucial component in increasing asphalt's self-healing, according to multiple studies. Asphalt will repair itself once it reaches the self-healing phase, which occurs at approximately 70° C and under resting conditions (resting from any load road)[15), 16), 17), 18)]. The heat transfer process has become a challenging research topic[19)]. During the

self-healing phase, asphalt or bitumen will be a Newtonian fluid capable of flowing into cracks[20), 21), 22)]. While 85 °C is the optimal temperature for self-healing asphalt, excessive heat will damage the asphalt rather than repair it. [15)]. Self-healing asphalt has been studied in several laboratories around the world since 1960. The microcrack in the asphalt can potentially have a longer service life if the researchers' hypothesis is correct[10)].

Asphalt can repair any damage that it sustains; however, it must be in a state of rest and not be moved by the load for this to occur. According to several studies, temperature has been shown to be the most critical factor in determining how quickly asphalt can recover from damage[3), 17), 18)]. Asphalt has a viscosity that increases with temperature[16)]. To increase the electrical conductivity of the asphalt mixture, it is necessary for the induction heating process. Increasing the asphalt's electrical conductivity and susceptibility to electromagnetic fields has been demonstrated to be the most effective technique to mend cracks[17)]. Increasing the temperature can boost the rate of self-healing, reducing the amount of time needed for asphalt to repair damage. Liu[18)] developed his study at Delft University using the induction heating technology to support this process. Induction heating is a technology that can heat conductive materials without necessarily direct contact of two objects which makes the heating processing can be both rapid and efficient. This is one of the most used heating technologies in the industrial sector.

In most cases, induction heating is achieved through power transformation from AC to DC to AC. A heating coil is provided with a voltage that is alternating at a high frequency by an AC. A magnetic field will be generated due to this current traveling through the workpiece or load object. As a result, two processes, namely magnetic hysteresis, and eddy currents, will heat the object being worked on[22)]. The induction heating system consists of a cooling system, a power source, and an induction coil. The properties of the heat generated are influenced by the coil winding, the coil diameter, the type of object being heated, the distance between the induction heater and the thing being heated, and the induction heater's configuration[19)].

Induction heating (IH) has become an indispensable technology in a variety of industries, including medical and residential heating applications. It possesses intrinsic advantages such as high efficiency, high power density, and low emissions. IH leverages the established principle of electromagnetic induction. Due to Joule's law of heating, the workpiece is heated by the eddy current created on the heating target. Therefore, the electromagnetic coupling and voltage transfer ratio between the coil and the workpiece are required parameters. In addition, the performance of the IH system depends on the geometry of the coil, the nature of the material, the frequency of the power supply, electrical conductivity, temperature, etc. With the development of power electronic converters, controlling the voltage transfer ratio and frequency in an IH system is straightforward[23-25)].

As a transmitter, a bifilar coil or tesla coil creates high voltage, high frequency, and low alternating current in combination to provide high-density flux. A bifilar coil functions slightly differently from a normal or monofilar coil. The ratio of turns in the winding determines the voltage gain in traditional transformers, when the winding is tightly linked. A bifilar coil technology that eliminates the requirement for a physical resonant capacitor in IH applications. The suggested system will lower the number of resonant elements, hence decreasing the size of the system as a whole. At frequencies exceeding the self-resonant frequency (SRF), the closed bifilar coil demonstrates series resonance. In contrast, the open bifilar coil has a series resonance at SRF and a parallel resonance at higher frequencies. In this study, closed bifilar is favored, and it is operated at a higher frequency than SRF to achieve series resonance and zero-voltage switching. The series resonance circuit will produce high electromagnetic resonance coupling, hence bolstering the magnetic field and increasing the efficiency[23)].

This study contributes on computational investigation to compare the ohmic loss and electromagnetic field asphalt values of identical shaped, diameter, wire spacing, and turn count monofilar and bifilar coils. The structure of the document is as follows: The second section explains the fundamentals of asphalt induction heating, whilst third section explains the methods. The results and analysis of the experiment simulation are discussed in Section 4. In Section 5, the major conclusions of the paper are presented.

2. State of the Art

As soon as it was determined that the increase in temperature was directly linked to the rate of healing, researchers began focusing on asphalt heating by induction. Unfortunately, induction heating is only possible on conductive materials, and asphalt is not one. Therefore, conductive components such as steel fiber are added to asphalt mixtures to boost the asphalt's total electrical conductivity[3), 17)].

Steel fiber is the most common addition used in the process of asphalt mending that employs induction heating[9)]. When Apostolidis[21)] evaluated the addition of electrical conductivity with steel fiber and iron powder as additives, he found that the addition of steel fiber increased electrical conductivity substantially more than the addition of iron powder. Additionally, tensile strength improves and prolongs the time until fatigue sets in. Apostolidis[21)] also noted that the effectiveness of induction heating rises as additive concentrations increase. However, there is a threshold beyond which the addition of chemicals will no longer result in a rise in temperature.

Liu[18)] also evaluated three separate types of steel fibers with diameters ranging from 29.6 to 191.1 micrometers, 8.89 to 12.7 micrometers, and 6.38 to 8.8 micrometers.

Using an induction heater with a frequency of 70 kHz and a power output of 50 kW, asphalt samples were heated. It was determined that longer steel fibers with smaller diameters functioned more effectively than shorter steel fibers with bigger diameters. The more intimate contact between the fibers results in an increase in conductivity. According to Liu's[18] findings, porous asphalt concrete has improved fatigue resistance and healing capacity, both of which boost the asphalt's durability. After being heated to 85 °C, the porous asphalt recovered dramatically after three hours of cooling. It is also found that the surface temperature of the samples is affected by the external environment, including wind speed and room temperature.

In their research, Garcia et al[3] . used samples of asphalt mixtures that were quite dense. Steel fiber with an average length of 1.5 millimeters and four different diameters ranging from 0.02855 millimeters to 0.03642 millimeters, 0.08389 millimeters, and 0.15498 millimeters. The combination comprises all four at concentrations of 2%, 4%, and 6% of the total bitumen content. At a maximum frequency of 78 kHz, an induction heating generator with a capacity of 30 kW was used to warm up each sample. At a temperature of 100° C, it was discovered that the damage could be repaired up to sixty percent. At a temperature of 500° C, a capillary flow of bitumen can be seen beginning between the cracks. Garcia found that the optimal strategy for obtaining optimum healing is to heat asphalt to a temperature above the Newtonian fluid transition and then maintain that temperature for a defined duration. Constant temperature must be maintained to prevent excessive heat loss to the surrounding environment.

Dai et al.[22] studied the self-healing capacity of asphalt materials using a peak-to-peak cyclic fracture test and assessed the influence that different temperatures of induction heating had on the healing capabilities of the asphalt mixture. By combining steel fiber type 1 with a length of 6.5 millimeters developed from Liu's study, t he samples were heated using a 5 kW induction heater with a frequency range from 0.120 to 0.160 MHz. It was discovered that the microcrack that had occurred had successfully recovered when the temperature was set to 60 degrees Celsius. The temperature of 100 degrees Celsius has been determined to be the one that facilitates the process of self-healing the best. Adding steel fibers makes it possible to recover cracks and achieve a high fracture strength. According to the references related to this field in Scopus database, it is possible to see that there was a discernible rise in the total number of publications in the field of self-healing asphalt between 2010 and 2018 (see Figure 1). In addition, 2022 marked the year with the highest number of articles published on self-healing asphalt, with 54 issued. Despite this, there was a drop in the total number of publications in both 2015 and 2019. On the other hand, this field has been around since 1986, but the self-healing method on asphalt was not published until 2014. It was, although it was first developed in 1987. The annual growth rate of the total number of publications was 1.89% over the previous 36 years.

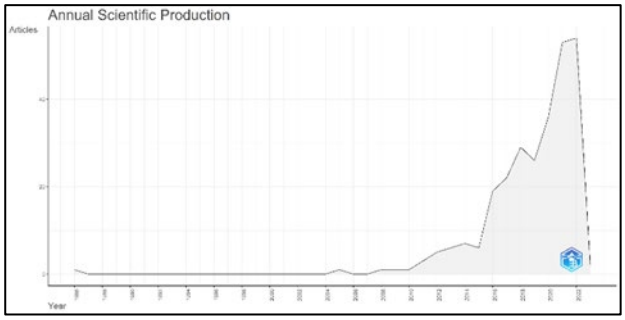

Fig. 1: Annual scientific production in self-healing method on asphalt

Therefore, conducting an analysis of references to different topics within this field can produce results that can make it simpler for readers to locate the appropriate references for the development of research within this field, and it can also make it possible to make predictions regarding topics that have not been thoroughly researched. For instance, additional research into new types of asphalt mixture that have improved self-healing capabilities has not yet reached a widespread level.

3. Fundamentals of Asphalt Induction Heating

3.1 Induction Heating

Induction heating is one of the most extensively utilized industrial heating methods. Low-frequency alternating current is converted to direct current and then back to high-frequency alternating current for a working coil to provide induction heating[26]. Due to eddy current and magnetic hysteresis phenomena, the conductive material will become heated[27]. The induction heater's coil winding, diameter, shape or geometry, type of conductive material, distance between them, and configuration can also affect the amount of heat generated[28].

Maxwell's equations guide the induction heating process by describing how eddy current is created in the workpiece. The produced head is depending on the intensity of the surrounding electromagnetic field. The Maxwell equation can be stated as follows:

$$\nabla \times \boldsymbol{H} = J + \frac{\partial \boldsymbol{D}}{\partial t} \text{ (Ampere's Law)} \quad (1)$$

$$\nabla \times \boldsymbol{E} = -\frac{\partial \boldsymbol{B}}{\partial t} \text{ (Faraday's Law)} \quad (2)$$

$$\nabla \cdot \boldsymbol{B} = 0 \text{ (Gauss's Law)} \quad (3)$$

$$\nabla \cdot \boldsymbol{D} = \rho \text{ (Gauss's Law)} \quad (4)$$

where, $\boldsymbol{H}$ represents the magnetic field intensity (A/m), $\boldsymbol{J}$ represents the electric current density associated with free charges (A/m^2), $\boldsymbol{B}$ represents the magnetic flux

density (weber/m^2), and $\boldsymbol{E}$ represents the electric field density (V/m). In addition, the parameters $\boldsymbol{H}$, $\boldsymbol{J}$, $\boldsymbol{B}$, and $\boldsymbol{E}$ follow these equations:

$$\boldsymbol{B} = \mu_0\mu_r\boldsymbol{H} \quad (5)$$

$$\mathbf{D} = \varepsilon_0\varepsilon_r\boldsymbol{E} \quad (6)$$

$$\boldsymbol{J} = \sigma\boldsymbol{E} \quad (7)$$

$$\sigma = 1/\rho \quad (8)$$

where $\varepsilon_r$represents relative permittivity, μ_r magnetic permeability, σ electrical conductivity of the material, and ρ electrical resistivity. In a vacuum, the permittivity value is expressed as 8.854×10^{-12} F/m. In contrast, permeability describes a material's capacity to conduct magnetic flux relative to a vacuum. $\mu_0 = 4\pi \times 10^{-7}$ H/m [29-31] represents the permeability value in a vacuum.

The temperature distribution of body workpiece can be expressed by following Fourier equation:

$$k\left(\frac{\partial^2 T}{\partial x^2} + \frac{\partial^2 T}{\partial y^2} + \frac{\partial^2 T}{\partial z^2}\right) + Q = \rho c \frac{\partial T}{\partial t} \quad (9)$$

Where, k is the thermal conductivity coefficient, Q is the intensity of the internal heat source owing to eddy current, c is the specific heat capacity of the workpiece, and ρ is the density. As a result of a quick increase in temperature, the surface may suffer significant variations in temperature[32-34].

3.2 Induction Heating on Asphalt

As mentioned previously, adjusting asphalt's temperature to optimal conditions can reduce the time needed for asphalt to recover from damage. Liu[17] researched induced heating-healing to create this condition. To reach optimum condition, conductive material or filler can be added to the asphalt mixture. The most common material used as an additive is steel fiber. This additive can increase the asphalt's overall electrical conductivity[35-37].

Several additive materials, such as steel fiber and iron powder, could be considered. Apostolidis[38] found in his study that steel fiber increased electrical conductivity significantly more than iron powder.

4. Methodology

This study compared the performance of induction coils with monofillar and bifillar constructions, as depicted in Figure 2.

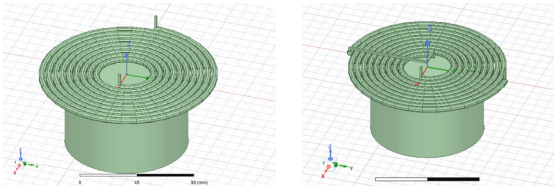

Fig. 2: (a) Monofilar and (b) Bifilar constructions[39]

Using the finite element method, the performance of monofilar and bifilar constructions was simulated using electrical simulations and thermal simulations. Figure 3 depicts the physical interaction between ANSYS Electronics Desktop and ANSYS Transient Thermal Analysis. The electrical simulation is performed first until the convergence value is reached, after which the results of the electrical simulation serve as the foundation for the thermal simulation.

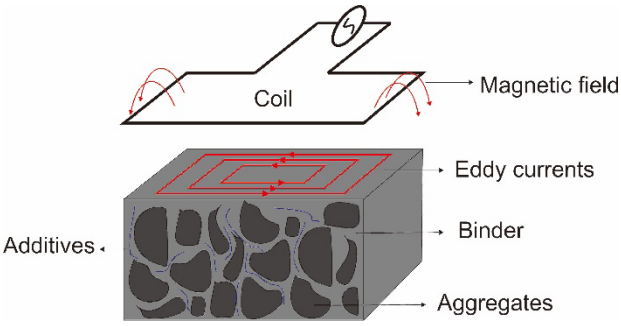

Fig. 3: Magnetic and thermal interaction scheme

In ANSYS Electronics Desktop, simplified models of monofilar and bifilar induction coil construction are created to reduce memory usage and computation time. Table 1 displays the design parameters for monofilar and bifilar constructs.

Table 1. Monofilar and bifilar coil specifications

Parameters	Monofilar	Bifilar
Turns	9	4.5 × 2
Diameter	140 mm	
Width	5 mm	5 mm
Thickness	0.1 mm	

In order to validate the performance of the two induction coil designs, an inductive asphalt component with a thickness of 60 mm and a diameter of 100 mm was added. As indicated in Figure 4, the inductive asphalt component is put beneath the induction coil at a distance of 2.5 mm. The inductive asphalt substance is asphalt with a steel fiber additive of 13.27%[2]. The electrical simulation of the induction coil and induction asphalt is performed by choosing the simulation parameters listed in Table 2.

Table 2. Simulation parameters for electrical analysis

Material	Inductive Asphalt	Copper
Mass density (Kg/m^3)	2360	8933
Relative Permittivity	6	1
Relative Permeability	1	0.999
Bulk Conductivity (S/m)	2100	58000000

Analyzing the ohmic loss value through electrical simulations utilizing the eddy current solution. The design geometry of the induction coil and induction asphalt is meshed at this simulation stage. The simulation input data parameters are frequency variations between 39 and 70 kHz at currents between 70 and 200 A. In this electrical simulation, it is assumed that the area surrounding the induction coil and induction asphalt is a vacuum, so that convection heat transfer to the air can be disregarded. The results of the electrical simulation are electromagnetic field and ohmic loss data which will be directly used as a basis for thermal simulations.

After the electrical simulation is completed, the electromagnetic field and ohmic loss data are used as internal heat generation parameters in the thermal simulation. The thermal simulation is performed by setting the initial temperature to 27 °C and applying boundary conditions in the form of heat transfer due to radiation, which is disregarded because the surrounding space is assumed to be a vacuum. The simulation is also limited for 900s to save memory usage. Table 3 displays the thermal simulation's parameters.

Table 3. Simulation parameters for thermal analysis

Material	Inductive Asphalt
Mass density (kg/m^3)	2360
Thermal conductivity (W/m·°C)	1,58
Specific heat (J/kg·°C)	920
Initial temperature (°C)	25 °C

5. Result and Discussion

5.1 Electrical Analysis

The electrical analysis determined electromagnetic field and ohmic loss distribution data encompassing the inductive asphalt. Figures 4 – 7 compare the distribution of electromagnetic fields between monofilar and bifilar constructions at frequencies of 39 kHz and 70 kHz and currents of 70 and 200 A. It can be seen from both figures that the maximum value of the electromagnetic field *H* is located in the middle of the top surface of inductive asphalt. In this location, the electromagnetic field can penetrate the asphalt's central surface area better than in other locations. The strength of an electromagnetic field is proportional to the current.

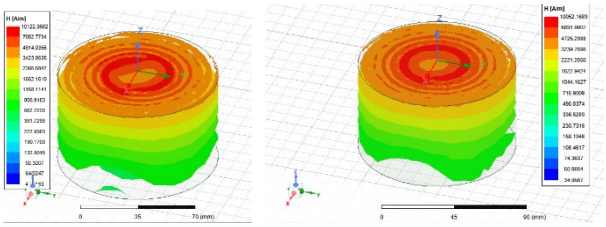

(a) bifilar (b) monofilar

Fig. 4: Comparison of the electromagnetic fields on asphalt with a current of 70 A and frequency of 39 kHz[39)]

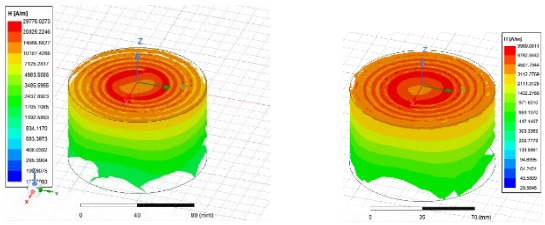

(a) bifilar (b) monofilar

Fig. 4: Comparison of the electromagnetic fields on asphalt with a current of 70 A and frequency of 70 kHz[39)]

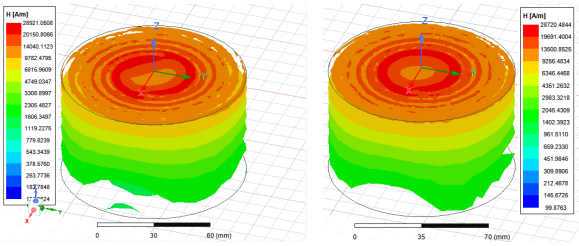

(a) bifilar (b) monofilar

Fig. 6: Comparison of the electromagnetic fields on asphalt with a current of 200 A and frequency of 39 kHz[39)]

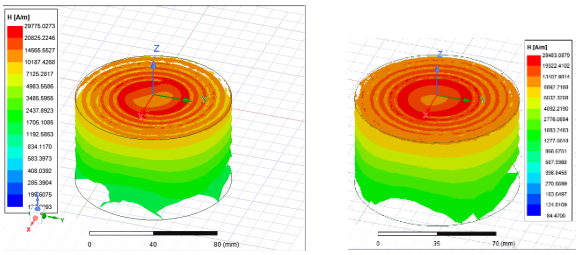

(a) bifilar (b) monofilar

Fig. 7: Comparison of electromagnetic fields on asphalt with a current of 200 A and frequency of 70 kHz[39)]

Figure 8 and 9 shows the comparison between the peak value of the electromagnetic field on monofilar and bifilar at 39 and 70 kHz respectively. It can be seen that the peak value electromagnetic field in both construction is increased when the magnitude of the current increased and the peak value of magnetic field in bifilar construction is slightly higher than the monofilar construction in every current magnitude. The other phenomenon that can be seen from Figures 8 and 9 are that the increasing of the frequency also has an effect on the increases of the magnitude of electromagnetic field in bifilar construction. At the same condition, monofilar reached lower

electromagnetic field values.

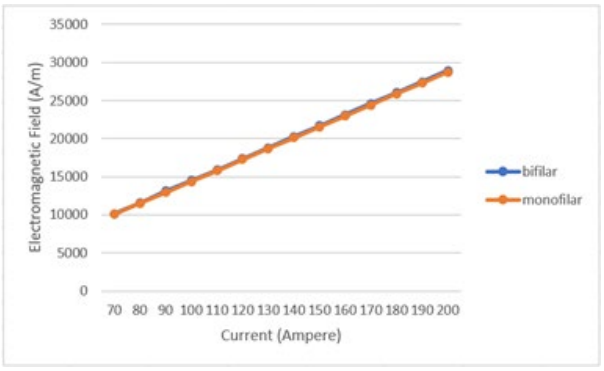

Fig. 8: Maximum value of the electromagnetic field at a frequency of 39 kHz

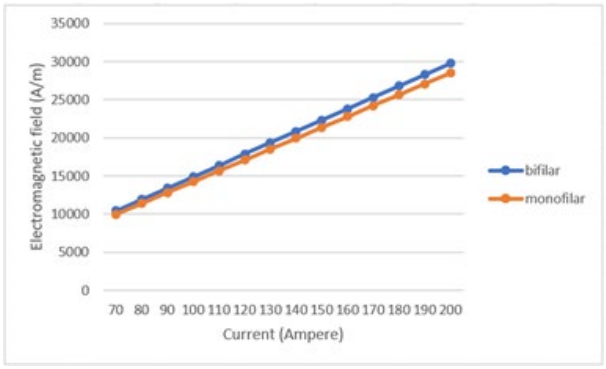

Fig. 9: Maximum value of the electromagnetic field at a frequency of 70 kHz

As shown in Figures 10– 13, the value of ohmic loss is greater at the outermost surface of inductive asphalt. It is possibly because the eddy current on the outermost surface is greater than that on the innermost surface. Along with the gradual decrease in its thickness, the ohmic loss is decreasing. The ohmic loss is also affected by the magnitude of the current and frequency; thus, the ohmic loss will increase as the magnitude of the current and frequency increases. This is because an increase in frequency causes an increase in power dissipation during each cycle. This power loss is used in the induction heating process.

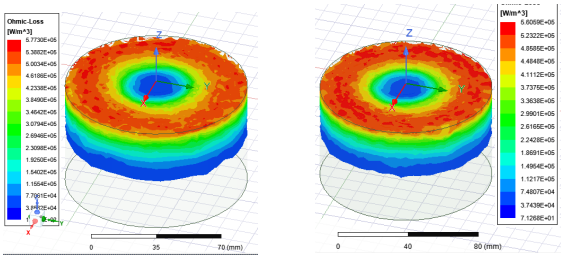

(a) bifilar (b) monofilar

Fig. 10: Comparison of the ohmic loss in asphalt with a current of 70 A and frequency of 39 kHz[39)]

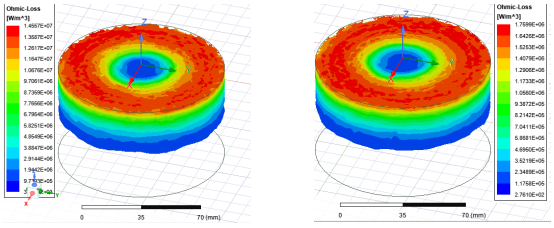

(a) bifilar (b) monofilar

Fig. 11: Comparison of the ohmic loss in asphalt with a current of 70 A and frequency of 70 kHz[39)]

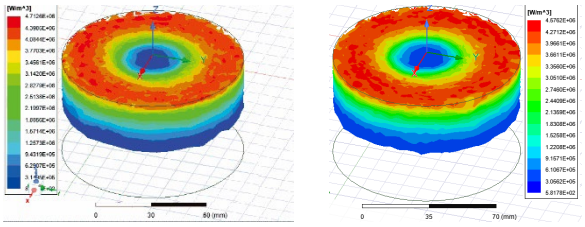

(a) bifilar (b) monofilar

Fig. 12: Comparison of the ohmic loss in asphalt with a current of 200 A and frequency of 39 kHz[39)]

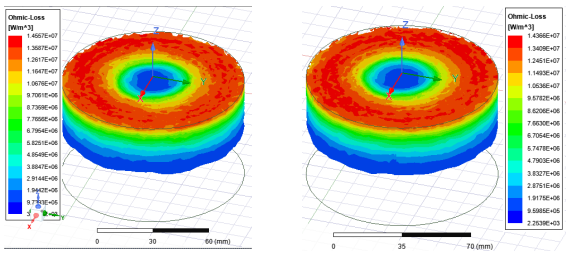

(a) bifilar (b) monofilar

Fig 13. Comparison of the ohmic loss in asphalt with a current of 200 A and frequency of 70 kHz[39)]

Figures 14 and 15 illustrate the peak value of the ohmic loss for monofilar and bifilar constructions at 39 and 70 kHz, respectively. In every frequency and current variation, the peak value of ohmic loss for the bifilar construction is slightly greater than for the monofilar construction. In both constructions, the peak value of ohmic loss at a frequency variation of 70 kHz is nearly three times greater than the variation at 39 kHz. The increase in generated ohmic loss is also affected by the increase in current. Due to the asphalt model's low magnetic properties, the hysteresis loss has a negligible impact and can be disregarded.

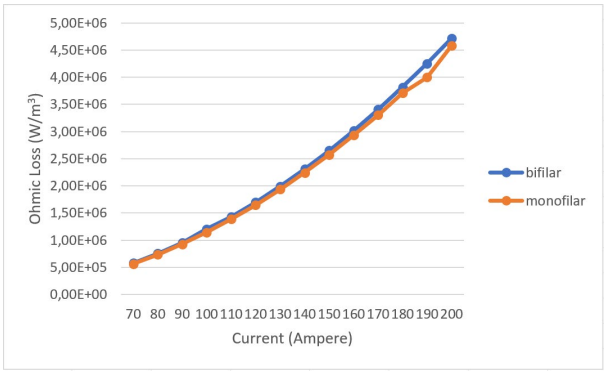

Fig. 14: Maximum value of the ohmic loss at a frequency of 39 kHz

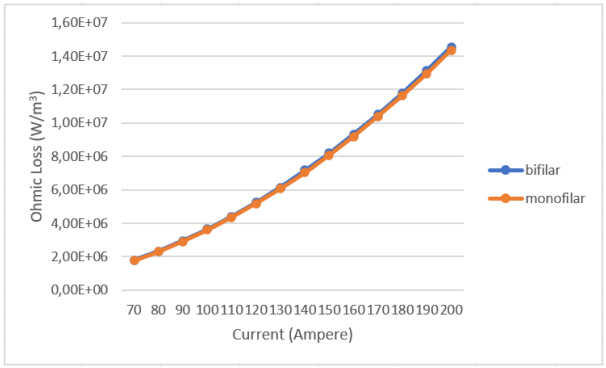

Fig. 15: Maximum value of the ohmic loss at a frequency of 70 kHz

5.2 Thermal Analysis

Thermal analysis is performed to determine the value of temperature distribution in every variation of currents and frequencies. Figure 16 compares the temperature and the current in the coil with a frequency of 39 kHz for monofilar and bifilar constructions. It can be seen that bifilar construction generates a slightly higher temperature than monofilar construction. At 190 to 200 A variations, the self-healing phase, which requires a temperature of 80 °C, can be reached within the first sixty seconds. However, if the desired self-healing temperature is to be reached rapidly, it will cost more to apply a larger current and generate additional power. However, if the power is restricted so that it can only generate a low current, it will take longer to reach the self-healing temperature. Although it will consume more time, the variation with lower currents does not require a great deal of power.

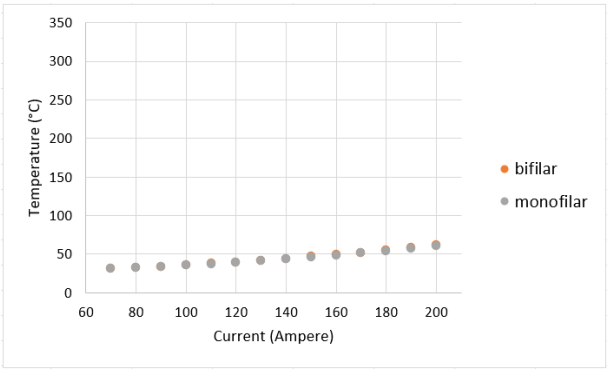

(a) At first 20 s

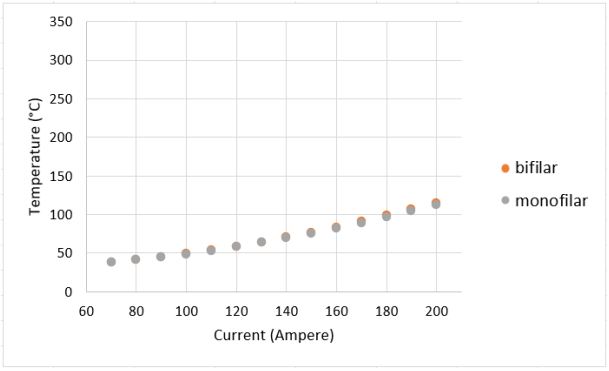

(b) At first 60 s

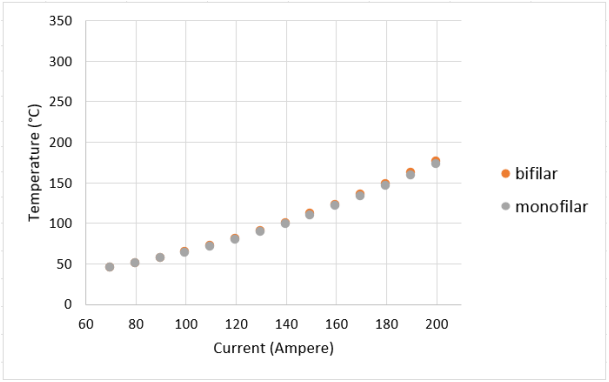

(c) At first 120 s

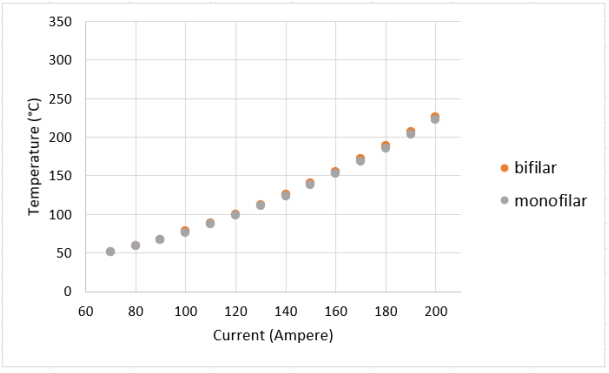

(d) At first 180 s

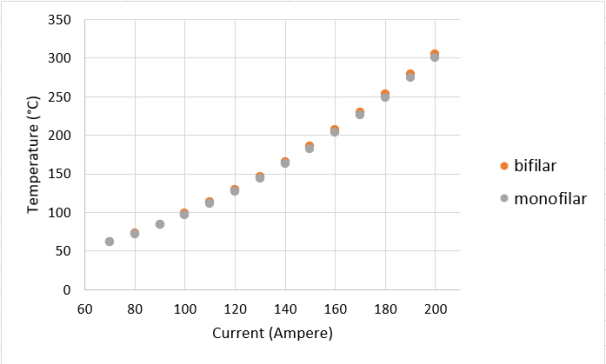

(e) At first 300s

Fig. 16: Comparison of currents and temperature distributions of inductive heating between bifilar and monofilar constructions on inductive asphalt at a frequency of 39 kHz

Figure 17 compares the temperature generated by monofilar and bifilar structures operating at a frequency of 70 kHz. From Figure 17, it is evident that the bifilar and monofilar constructions do not generate temperatures differently. However, higher frequencies have an effect on the rise in heat production. On a frequency of 70 kHz, the self-healing temperature can be reached in just 20 seconds with a current magnitude of 150 A. The time and current required to achieve the desired temperature are considerably less than the 39 kHz variation. The higher frequency generates a larger electromagnetic field, allowing the ohmic loss generation on the induction asphalt to be optimized.

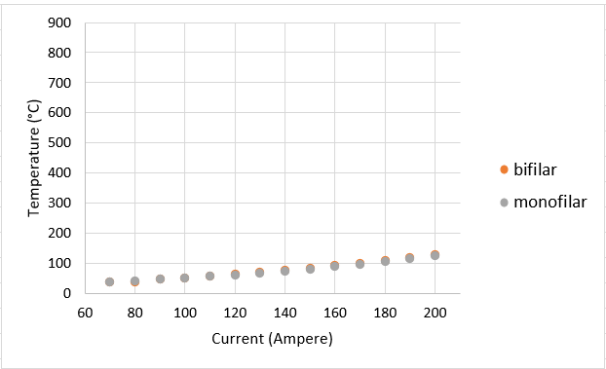

(a) At first 20 s

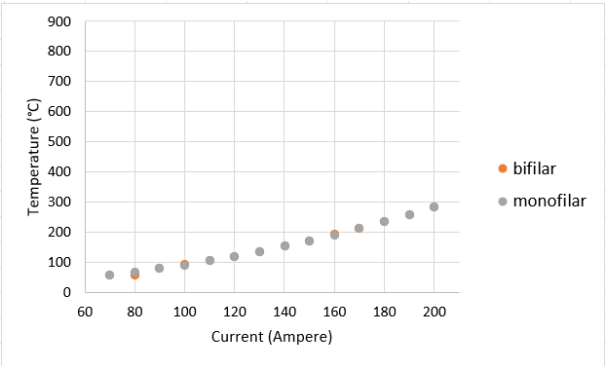

(b) At first 60 s

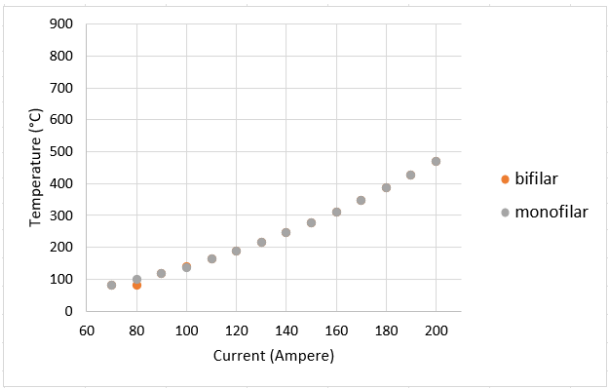

(c) At first 120 s

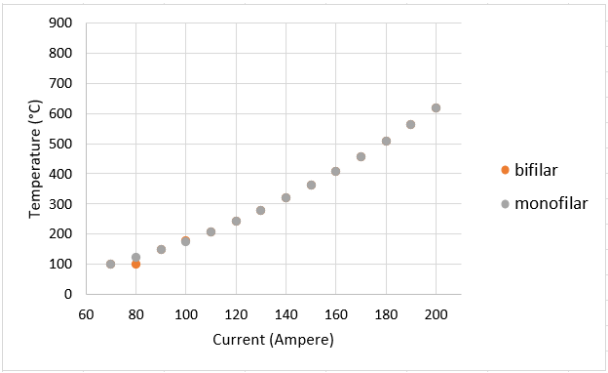

(d) At first 180 s

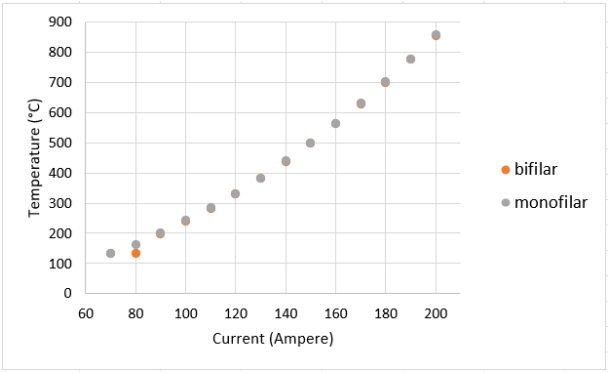

(e) At first 300s

Fig 17. Comparison of currents and temperature distributions of inductive heating between bifilar and monofilar constructions on asphalt inducted at a frequency of 70 kHz

In general, a bifilar coil has its potential for asphalt rejuvenation due to some advantages instead of monofillar. The advantages of a bifilar coil over an unifilar coil include:

- **Increased Inductance**: The inductance of a bifilar coil is higher than that of an unifilar coil. This is because the two wires in a bifilar coil are wound together, which increases the magnetic field strength and the amount of energy that can be stored.
- **Reduced Resistance**: The resistance of a bifilar coil is lower than that of an unifilar coil because the two wires in a bifilar coil are wound together. This reduces the amount of wire that is needed, which lowers the resistance and improves the efficiency of

the coil.

- **Improved Frequency Response**: A bifilar coil has a wider frequency response than an unifilar coil because the two wires in a bifilar coil are wound together, which reduces the parasitic capacitance and inductance of the coil. This improves the coil's ability to respond to high-frequency signals.
- **Reduced Noise**: A bifilar coil can reduce the noise in a circuit because the two wires are wound together in the same direction. This cancels out any external electromagnetic interference, which can reduce the amount of noise in the circuit.

5. Conclusion

This research concludes that induction heating is a viable alternative or self-healing method for asphalt. The performance of the induction heating that occurs is also affected by the coil's geometric shape. After considering the results of the simulations conducted, the following conclusions were reached:

(1) Induction heaters with bifilar coils produce a slightly greater ohmic-loss than monofilar, as the bifilar area is slightly larger for the same number of turns.
(2) The magnetic field intensity, H, (A/m), the value produced by a bifilar coil is also slightly greater than that produced by a monofilar coil.
(3) Monofilar and bifilar do not provide significat differences in time to reach 80 or even the current / frequency required to produce the minimum temperature of 80. Nevertheless, bifilar induction heating results in a slightly higher bitumen surface temperature, as well as higher ohmic-loss and H values, compared to monofilar induction heating.
(4) This condition can repair asphalt microcracks, but it is insufficient to repair asphalt damage in the deeper layers.
(5) Depending on how quickly the optimal self-healing temperature (80 °C) must be reached, various combinations of current and frequency can be used.

Further research is still needed to develop this self-healing asphalt method because even though the bifilar coil gives a slightly higher performance, the ease and cost of manufacturing must certainly be a further consideration in the future.

Acknowledgements

This research was totally supported by Universitas Sebelas Maret through Hibah Unggulan Terapan 2023, LPPM UNS

Nomenclature

$\boldsymbol{H}$	magnetic field intensity (A/m)
$\boldsymbol{J}$	conduction current density (A/m^2),
$\boldsymbol{E}$	electric field intensity (V/m)
$\boldsymbol{B}$	magnetic flux density (weber/m^2)
$\boldsymbol{D}$	electric flux density (C/m^2)

Greek symbols

∇	nabla
ε	permittivity relative
μ	permeability magnetic
σ	electrical conductivity of the material

References

1) S. Xu, A. García, J. Su, Q. Liu, A. Tabaković, and E. Schlangen, "Self-Healing Asphalt Review: From Idea to Practice," *Adv. Mater. Interfaces*, vol. 5, no. 17, pp. 1–21, 2018, doi: 10.1002/admi.201800536.
2) A. Menozzi, A. Garcia, M. N. Partl, G. Tebaldi, and P. Schuetz, "Induction healing of fatigue damage in asphalt test samples," *Constr. Build. Mater.*, vol. 74, pp. 162–168, 2015, doi: 10.1016/j.conbuildmat.2014.10.034.
3) Á. García, E. Schlangen, M. Van De Ven, and D. Van Vliet, "Induction heating of mastic containing conductive fibers and fillers," *Mater. Struct. Constr.*, vol. 44, no. 2, pp. 499–508, 2011, doi: 10.1617/s11527-010-9644-2.
4) Hamdi, S. P. Hadiwardoyo, A. G. Correia, and P. Pereira, "Pavement Maintenance Optimization Strategies for National Road Network in Indonesia Applying Genetic Algorithm," *Procedia Eng.*, vol. 210, pp. 253–260, 2017, doi: 10.1016/j.proeng.2017.11.074.
5) A. Garcia, S. Salih, and B. Gómez-Meijide, "Optimum moment to heal cracks in asphalt roads by means electromagnetic induction," *Constr. Build. Mater.*, vol. 238, p. 117627, 2020, doi: 10.1016/j.conbuildmat.2019.117627.
6) Q. Ahsan, W. T. Hui, I. S. Othman, L. P. Jun, and A. Putra, "Preparation and characterization of natural fiber filled asphalt based damping material," *J. Adv. Res. Fluid Mech. Therm. Sci.*, vol. 47, no. 1, pp. 8–15, 2018.
7) I. Choirunisa, Ubaidillah, F. Imaduddin, and E. T. Maharani, "MR Damper Modeling using Gaussian and Generalized Bell of ANFIS Algorithm," Journal of Novel Carbon Resource Sciences & Green Asia Strategy, Vol. 08, Issue 03, pp673-685, September 2021
8) A. Arunika, J. F. Fatriansyah, and V. A. Ramadheena, "Detection of Asphalt Pavement Segregation Using Machine Learning Linear and Quadratic Discriminant Analyses," Journal of Novel Carbon Resource Sciences & Green Asia Strategy, Vol. 09,

Issue 01, pp 213-218, March 2022.
9) K.G. Swapan, Self-healing Materials: Fundamentals, Design Strategies, and Applications, John Wiley and Sons, 2008.
10) P. Ayar, F. Moreno-Navarro, and M. C. Rubio-Gámez, "The healing capability of asphalt pavements: A state of the art review," *J. Clean. Prod.*, vol. 113, pp. 28–40, 2016, doi: 10.1016/j.jclepro.2015.12.034.
11) J. L. Concha and J. Norambuena-Contreras, "Thermophysical properties and heating performance of self-healing asphalt mixture with fibres and its application as a solar collector," *Appl. Therm. Eng.*, vol. 178, p. 115632, 2020, doi: 10.1016/j.applthermaleng.2020.115632.
12) Á. García, E. Schlangen, and M. Van De Ven, "Properties of capsules containing rejuvenators for their use in asphalt concrete," *Fuel*, vol. 90, no. 2, pp. 583–591, 2011, doi: 10.1016/j.fuel.2010.09.033.
13) B. R. Anupam, U. C. Sahoo, and A. K. Chandrappa, "A methodological review on self-healing asphalt pavements," *Constr. Build. Mater.*, vol. 321, no. December 2021, p. 126395, 2022, doi: 10.1016/j.conbuildmat.2022.126395.
14) D. Sun *et al.*, "A comprehensive review on self-healing of asphalt materials: Mechanism, model, characterization and enhancement," *Adv. Colloid Interface Sci.*, vol. 256, pp. 65–93, 2018, doi: 10.1016/j.cis.2018.05.003.
15) M. M. Karimi, S. Amani, H. Jahanbakhsh, B. Jahangiri, and A. H. Alavi, "Induced heating-healing of conductive asphalt concrete as a sustainable repairing technique: A review," *Clean. Eng. Technol.*, vol. 4, no. February, p. 100188, 2021, doi: 10.1016/j.clet.2021.100188.
16) A. Garcia, E. Schlangen, and M. Van de Ven, "Two ways of closing cracks on asphalt concrete pavements: Microcapsules and induction heating," *Key Eng. Mater.*, vol. 417–418, pp. 573–576, 2010, doi: 10.4028/www.scientific.net/KEM.417-418.573.
17) Q. Liu, W. Yu, E. Schlangen, and G. Van Bochove, "Unravelling porous asphalt concrete with induction heating," *Constr. Build. Mater.*, vol. 71, pp. 152–157, 2014, doi: 10.1016/j.conbuildmat.2014.08.048.
18) K. Liu, C. Fu, P. Xu, S. Li, and M. Huang, "An eco-friendliness inductive asphalt mixture comprising waste steel shavings and waste ferrites," *J. Clean. Prod.*, vol. 283, no. xxxx, p. 124639, 2021, doi: 10.1016/j.jclepro.2020.124639.
19) C. Sulochana and T. P. Kumar, "Heat Transfer of SWCNT-MWCNT Based Hybrid Nanofluid Boundary Layer Flow with Modified Thermal Conductivity Model," *J. Adv. Res. Fluid Mech. Therm. Sci.*, vol. 92, no. 2, pp. 13–24, 2022, doi: 10.37934/arfmts.92.2.1324.
20) Á. García, "Self-healing of open cracks in asphalt mastic," *Fuel*, vol. 93, pp. 264–272, 2012, doi: 10.1016/j.fuel.2011.09.009.
21) P. Apostolidis, Mixes INDUCTION HEATING IN ASPHALT MIXES, (2015) 130. https://doi.org/10.13140/ RG.2.2.20606.28480.
22) D. Grossegger and A. Garcia, "Influence of the thermal expansion of bitumen on asphalt self-healing," *Appl. Therm. Eng.*, vol. 156, no. March, pp. 23–33, 2019, doi: 10.1016/j.applthermaleng.2019.04.034.
23) D. Grossegger, B. Gomez-Meijide, S. Vansteenkiste, and A. Garcia, "Influence of rheological and physical bitumen properties on heat-induced self-healing of asphalt mastic beams," *Constr. Build. Mater.*, vol. 182, pp. 298–308, 2018, doi: 10.1016/j.conbuildmat.2018.06.148.
24) P. Vishnuram and G. Ramachandiran, "Capacitor-less induction heating system with self-resonant bifilar coil," *Int. J. Circuit Theory Appl.*, vol. 48, no. 9, pp. 1411–1425, 2020, doi: 10.1002/cta.2830.
25) D. P. Da Silva and S. F. Pichorim, "Modeling of open square bifilar planar spiral coils," *J. Microwaves, Optoelectron. Electromagn. Appl.*, vol. 17, no. 3, pp. 319–339, 2018, doi: 10.1590/2179-10742018v17i31254.
26) P. Vishnuram, G. Ramachandiran, T. S. Babu, and B. Nastasi, "Induction heating in domestic cooking and industrial melting applications: A systematic review on modelling, converter topologies and control schemes," *Energies*, vol. 14, no. 20, 2021, doi: 10.3390/en14206634.
27) O. Lucia, P. Maussion, E. J. Dede, and J. M. Burdio, "Induction heating technology and its applications: Past developments, current technology, and future challenges," *IEEE Trans. Ind. Electron.*, vol. 61, no. 5, pp. 2509–2520, 2014, doi: 10.1109/TIE.2013.2281162.
28) H. M. El-Mashad and Z. Pan, "Application of Induction Heating in Food Processing and Cooking," *Food Eng. Rev.*, vol. 9, no. 2, pp. 82–90, 2017, doi: 10.1007/s12393-016-9156-0.
29) H.M. El-Mashad, and Z. Pan, "Application of induction heating in food processing and cooking," *Food Eng. Rev.*, **9** (*2*) 82–90 (2017). doi:10.1007/s12393-016-9156-0.
30) S. Singh, S. K. Singh, R. Kumar, A. Shrama, and S. Kanga, "Finding Alternative to River Sand in Building Construction," Journal of Novel Carbon Resource Sciences & Green Asia Strategy, Vol. 09, Issue 04, pp973-992, December 2022
31) R. Sun, Y. Shi, Z. Pei, Q. Li, and R. Wang, "Heat transfer and temperature distribution during high-frequency induction cladding of 45 steel plate," *Appl. Therm. Eng.*, vol. 139, no. August 2017, pp. 1–10, 2018, doi: 10.1016/j.applthermaleng.2018.04.100.
32) M. N. Z. Abidin and M. Y. Misro, "Numerical Simulation of Heat Transfer using Finite Element Method," *J. Adv. Res. Fluid Mech. Therm. Sci.*, vol. 92, no. 2, pp. 104–115, 2022, doi: 10.37934/arfmts.92.2.104115.

33) A. R. Ismail, N. Jusoh, R. M. Zein, I. A. Rahman, M. A. M. Asri, and N. K. Makhtar, "Application of computational fluid dynamic simulation for the study of heat stress and heat strain-A review," *J. Adv. Res. Fluid Mech. Therm. Sci.*, vol. 73, no. 2, pp. 138–145, 2020, doi: 10.37934/ARFMTS.73.2.138145.
34) H. T. Alkasasbeh, "Numerical Solution of Heat Transfer Flow of Casson Hybrid Nanofluid over Vertical Stretching Sheet with Magnetic Field Effect," *CFD Lett.*, vol. 14, no. 3, pp. 39–52, 2022, doi: 10.37934/cfdl.14.3.3952.
35) B. Gómez-Meijide, H. Ajam, A. Garcia, and S. Vansteenkiste, "Effect of bitumen properties in the induction healing capacity of asphalt mixes," *Constr. Build. Mater.*, vol. 190, pp. 131–139, 2018, doi: 10.1016/j.conbuildmat.2018.09.102.
36) Á. García, E. Schlangen, M. Van De Ven, and Q. Liu, "A simple model to define induction heating in asphalt mastic," *Constr. Build. Mater.*, vol. 31, pp. 38–46, 2012, doi: 10.1016/j.conbuildmat.2011.12.046.
37) H. Li, J. Yu, Q. Liu, Y. Li, Y. Wu, and H. Xu, "Induction Heating and Healing Behaviors of Asphalt Concretes Doped with Different Conductive Additives," *Adv. Mater. Sci. Eng.*, vol. 2019, 2019, doi: 10.1155/2019/2190627.
38) P. Apostolidis, "EXPERIMENTAL AND NUMERICAL INVESTIGATION OF INDUCTION HEATING IN ASPHALT MIXES," no. November 2015, p. 130, 2015, doi: 10.13140/RG.2.2.20606.28480.
39) A. Esdiyanto, U. Ubaidillah, E. P. Budiana, S. Sangadji, B.W. Lenggana, "Simulation Analysis of Induction Heating as a Self-Healing Method on Asphalt," CFD Letters, Vol. 15 (3), 2023, doi: 10.37934/cfdl.15.3.4865.